FLEXSTAB - A COMPUTER PROGRAM FOR THE PREDICTION OF LOADS AND STABILITY AND CONTROL OF FLEXIBLE AIRCRAFT

Brian R. Perkin
Boeing Aerospace Company

Larry L. Erickson
NASA Ames Research Center

SUMMARY

This paper describes and illustrates capabilities of the FLEXSTAB Computer Program System. FLEXSTAB is a system of computer programs for performing aeroelastic analysis of a wide variety of current and future aircraft configurations. There are two versions of FLEXSTAB: a NASA controls-fixed version* identified as Level 1 FLEXSTAB; and an Air Force version,** identified as Level 2 FLEXSTAB, which provides for active controls analysis at low frequencies. The aerodynamic theory used in FLEXSTAB is applicable to both steady and unsteady, subsonic and supersonic flow for multiple wing-body-tail-nacelle configurations with a plane of symmetry. For unsteady flow calculations, an unsteady aerodynamic theory is used which is appropriate for the low reduced frequencies associated with aircraft flight dynamics. The aircraft may be modeled as either a rigid or flexible structure. FLEXSTAB will trim the aircraft in steady reference flight and compute both static and dynamic stability and control derivatives and the stability behavior about the trim condition. The airplane lifting pressure distribution, aerodynamic and inertia loads and deflected shape are also computed.

INTRODUCTION

FLEXSTAB is a system of computer programs for performing aeroelastic analysis of a wide variety of current and future aircraft configurations. There are two versions of FLEXSTAB: a NASA, controls-fixed version, identified as Level 1 FLEXSTAB (ref. 1 and 2); and an Air Force version, identified as Level 2 FLEXSTAB (ref. 3), which provides for active controls analysis at low frequencies. Effort is currently underway to consolidate these two versions into a Level 3 FLEXSTAB program. This paper describes the NASA version of FLEXSTAB in some detail with a brief description of the Air Force version.

---

* Sponsored by NASA Ames under Contracts NAS2-5006 and NAS2-7729.
** Sponsored by the Air Force Flight Dynamics Laboratory under Contracts F33615-72-C-1172 and F-33615-75-C-3132.

The degree to which aeroelasticity influences aircraft flight behavior, such as stability or controllability and structural loads, varies greatly from aircraft to aircraft, depending upon configuration and performance requirements. Obviously the aeroelastic effects become more significant with the trend to lighter weight, more flexible aircraft structures. The low aspect ratio, thin wing, slender body configurations of large supersonic aircraft are a prime example. The aeroelastic effects for this class of aircraft arise from complex structural deformation shapes (relative to higher aspect ratio configurations) affecting both the loads and the stability. Further, because some of their structural motions may have characteristic frequencies approaching those of their rigid body motions, dynamic stability may be significantly affected by the dynamics of the structure through aerodynamic coupling between the rigid body and structural motions.

In recognition of these needs, NASA, and later the U.S. Air Force, sponsored the development of the FLEXSTAB computer programs. These are regarded as first generation programs which partially satisfy the need for an automated aeroelastic analysis tool.

This paper presents a brief introduction to the capabilities and limitations of the FLEXSTAB programs. Some of the capabilities are illustrated by results from application of FLEXSTAB to actual and proposed aircraft configurations including the YF-12A aircraft, the NASA Arrow-Wing Supersonic Cruise Aircraft, and the Boeing Fixed-Wing SST.

FLEXSTAB CAPABILITIES

The NASA Level 1 FLEXSTAB is a system of fourteen separate computer programs (totalling about 100 000 source statements) using linear theories to evaluate controls-fixed static and dynamic stability, trim state, inertial and aerodynamic loading, and elastic deformations of aircraft configurations at subsonic and supersonic speeds. The functional configuration of Level 1 FLEXSTAB is shown in figure 1. A wide range of analysis capability has been incorporated into the FLEXSTAB system as shown in table 1. A typical analysis sequence is shown in figure 2.

The aerodynamic theory is applicable to both steady and unsteady, subsonic and supersonic flow for multiple wing-body-tail-nacelle configurations with a plane of symmetry. The aerodynamic theory is a linearized potential flow theory and contains a low frequency approximation to unsteady flow. A single aerodynamic paneling scheme can be used for steady and unsteady, subsonic and supersonic flow. Structural flexibility and inertial properties are modeled using an elastic axis representation with beam finite elements (internal to FLEXSTAB). Also, structural properties generated externally by programs such as NASTRAN® or ATLAS can be interfaced with FLEXSTAB where a better structural definition is required, such as for low aspect ratio aircraft. Structural and aerodynamic properties are integrated using a mean-axis representation. The

dynamics of a flexible aircraft are resolved into structural dynamic free vibration modes superimposed on rigid body dynamics. The equations of motion are expressed for a steady, reference motion to determine trim and static stability, inertial and aerodynamic loading, and elastic deformations. They are also expressed in terms of unsteady perturbations about the reference motion to determine dynamic stability by characteristic roots or by time histories following an initial perturbation or following penetration of a discrete gust flow field. A brief description of these capabilities with corresponding limitations follows.

FLEXSTAB AERODYNAMIC MODELING

Geometry

The user inputs the aerodynamic geometry of a symmetric configuration as a series of slender bodies with interference surfaces and thin surfaces as shown in figure 3. A fuselage, a nacelle, or an external store is represented by a slender body of revolution. The body camber is defined as camber slopes with respect to a straight aerodynamic mean centerline, and the boundary conditions are set up on a cylindrical surface of revolution. This aerodynamic mean centerline also defines the elastic axis for the body. Interference effects on a slender body are accounted for by an interference shell which is a cylinder of constant polygonal cross section. A wing, horizontal tail, vertical tail, or any other lifting surface (including control surfaces) is represented by linearization of the boundary conditions about a mean plane.

Aerodynamics

The aerodynamic influence coefficient method used in FLEXSTAB to solve the linearized potential flow equations is an extension of the constant pressure paneling technique due to Woodward (ref. 4). For each of the components in the aerodynamic model, FLEXSTAB computes aerodynamic influence coefficient matrices which relate pressure at one aerodynamic panel to the flow incidence and incidence rates of another panel. Incidence angles are expressed in terms of the configuration geometry (involving camber, twist, thickness, dihedral, control surface deflection), aircraft attitude and motion, and elastic deformations. The flow boundary conditions are the flow incidences. Interference effects between thin bodies and slender bodies are approximately accounted for by vortex panels on the thin bodies and by interference surfaces (shells) enclosing each slender body.

For unsteady flow calculations, an unsteady aerodynamic theory is used which is appropriate for the low reduced frequencies associated with aircraft flight dynamics. The theory is not intended to deal with high frequency motion such as encountered in flutter or dynamic loads due to atmospheric turbulence (fig. 4). The unsteady flow model is unique in that it has the same three-dimensional capability as the steady flow model at both supersonic and subsonic speeds ... a feature not found in other unsteady formulations.

Also, unlike other supersonic schemes such as the Mach Box method, the FLEXSTAB aerodynamic model does not require the introduction of "diaphragm regions" for wings with subsonic edges.

Nonlinear and viscous effects are not accounted for analytically since the aerodynamic formulation is based on linearized potential flow theory. The severity of these limitations is a function of the configuration and flight condition. To partially alleviate this limitation, provision has been made for incorporating user specified changes to the aerodynamic matrices, flow incidence vectors, aerodynamic force and moment coefficients, and lifting pressure distributions.

FLEXSTAB STRUCTURAL MODELING

The user can model the aircraft either as a rigid or flexible structure. For a flexible structure, two modeling options are available (see fig. 5). If the structure is amenable to an elastic axis idealization, an internal structures program using beam type finite-elements is provided. In this case, the user supplies FLEXSTAB with the elastic axis geometry, and stiffness (EI, GJ) and mass information.

For elastic modeling of complex structures, FLEXSTAB will accept the structural output of external finite element programs such as NASTRAN® or ATLAS (fig. 6). In this case, a general three-dimensional model must be "reduced" to an equivalent representation consistent with the FLEXSTAB aerodynamic model. That is, the flexibility and inertia definitions are reduced to structural nodes located on the mean aerodynamic plane of thin bodies and on the mean aerodynamic centerlines of slender bodies (fig. 5).

A flexible structure can be represented in either of two ways.

1. Static-Elastic - The structural deformations are assumed to occur statically, and all effects due to structural vibration are ignored. Using this assumption, the structural deformations are related to the applied loads by the flexibility matrix of the unrestrained vehicle and are in phase with the rigid body motion.

2. Residual-Elastic - The structural dynamic motion is accounted for by using the free-vibration-mode shape amplitudes as structural degrees of freedom. FLEXSTAB uses the "residual flexibility" technique, whereby the dynamic effects of just the lower frequency modes (which are most likely to couple with the rigid body motion) are retained. The dynamic effects of the higher frequency modes are neglected, but their static flexibility effects are retained (hence the name residual flexibility). The frequencies of the retained modes must not violate the low frequency approximation of the unsteady aerodynamics.

In both cases the inertial relief is included in the flexibility matrix which is then transformed to the mean-axis system. The static-elastic approach is used for the trim and static stability problems; also, it is usually quite adequate for dynamic stability cases in which the lowest structural vibration frequency is relatively far removed from the frequency of the aircraft short-period motion. The residual flexibility technique is provided for analyzing dynamic stability problems in which the lower structural frequencies and the short-period aircraft motion may be close enough together to significantly couple the aircraft "rigid" body and structural dynamic motion.

In general, the present FLEXSTAB versions are not applicable to dynamic loads analysis. This is because of the low reduced frequency approximation used for the unsteady aerodynamics and the simplifications made in the structural dynamic model. The structural simplifications define the fuselage mass and stiffness along a straight line elastic axis and neglect all rotary inertia terms, (fig. 7). For a wing surface, a dumbbell mass representation is used to represent the wing panel inertial properties.

PROBLEM ANALYSIS

The aerodynamic and structural representations are combined into an aeroelastic set of equations which govern the aircraft loads and flight behavior. Except for the time histories response and the postprocessing of the loads, solutions to these equations are computed in the Stability Derivatives and Static Stability (SD&SS) program. Figure 8 presents a schematic of the SD&SS program illustrating the user input including the empirical data and the program output. The basic calculations for the trim solution and stability and control are further described below.

Trim Solution

From user specified values of steady reference flight conditions (load factor or pitch rate, flightpath angle or thrust, yaw and roll rates, bank angle, and altitude or speed and dynamic pressure), FLEXSTAB computes the trim parameters and trimmed force coefficients shown in table 2. Three solution options are available:

1. Trim solution with constant coefficients: Here, all the aerodynamic force coefficients are computed analytically by FLEXSTAB, and the trim parameters are obtained directly from the linearized equations of motion.

2. Iterative trim solution: In this case the user can supply a table of nonlinear force and moment coefficients to replace all or a portion of the FLEXSTAB computed rigid aerodynamic coefficients; aeroelastic increments to these coefficients are computed on the basis of linear theory.

3. User specified trim parameters: This option allows the user to specify values for the trim parameters, thus, in general leaving the aircraft in an unbalanced load condition. This option is useful for calculating loads per unit control surface deflection, for specifying untrimmed flight maneuvers, or for matching rigid model wind tunnel test conditions.

After the trim variables are obtained (or specified), FLEXSTAB computes lifting pressure distributions, aerodynamic and inertial loads at aerodynamic centroids, and elastic deflections due to these loads. In addition, for steady symmetric flight, the aerodynamic pressures can be integrated over user specified portions of the aircraft to obtain shear, bending, and torque reactions to the applied airloads (ALOADS program) when the structural model originates from an external finite element program.

Stability and Control Calculations

The FLEXSTAB analysis proceeds by perturbing the aircraft motion variables (both rigid and elastic) about their values for the reference flight condition. This results in explicit matrix equations from which the static and dynamic stability and control derivatives are computed. These derivatives, listed in tables 3 and 4, are computed for both longitudinal and lateral directional motions. The linearized flow equations used in FLEXSTAB govern first order aerodynamic effects; second-order nonlinear terms, such as the product of angle of attack with angle of sideslip, are neglected. For small dihedral configurations these second-order terms can significantly affect the yaw rate and sideslip stability derivatives (ref. 5).

The stability characteristics about the reference condition are computed for two cases, 1. static (steady state flight), and 2. dynamic, (time varying motion of the aircraft). For the static case, the static stability parameters listed in table 2 are computed. For the dynamic case, the aircraft stability behavior is determined with controls fixed. (In the Air Force version of FLEXSTAB, reference 3, the low frequency dynamics of vehicles with feedback controls and sensors can be evaluated). Using the linearized equations of motion, the roots of the corresponding characteristic equation are computed. These roots in turn supply the dynamic modes of motion together with the associated frequencies and damping coefficients. Each real root and each oscillatory pair of roots are described individually. For each mode the following is printed:

- Times and number of cycles to one-half (or double) and one-tenth amplitude
- Frequency and period
- Logarithmic decrement and ratio of successive maximum displacement

- Undamped natural frequency
- Damping ratio
- Phase and amplitudes of modal coupling terms

Time Histories Response

The nonlinear perturbation equations of motion are numerically integrated using a Runge-Kutta procedure to determine the time histories response. The time histories response is required when the user wants to investigate the dynamic stability due to; (a) the large perturbations to motion variables, and (b) a discrete gust. Three types of discrete gust inputs may be specified, these are sine, 1-cosine, and modified square wave. Nonlinear aerodynamic data may be input as a tabular series for calculating the response. Specification of the discrete gust must be consistent with the limitation of the low frequency approximation.

APPLICATIONS OF LEVEL 1 FLEXSTAB

Some of the capabilities of FLEXSTAB are illustrated by the results from application to different airplane configurations. The NASA Arrow-Wing Supersonic Cruise Aircraft has been used to illustrate the prediction of stability and control parameters for the rigid and flexible airplane. Also, comparisons between FLEXSTAB results and results from other analysis tools, wind tunnel tests, and flight data are presented for the YF-12A, an Arrow-Wing–Body configuration, the Boeing Fixed-Wing SST, and the Space Shuttle Orbiter. The YF-12A results are for a flexible aircraft and the other three for rigid aircraft.

NASA Arrow-Wing Supersonic Cruise Aircraft

This configuration was used by Boeing in support of the NASA SCAR program (ref. 6). In that program FLEXSTAB was used to determine the aeroelastic loads using elastic properties supplied by the ATLAS finite-element structural analysis program. FLEXSTAB has also been used to predict the stability and control parameters for the configuration. Figure 9 shows the aerodynamic paneling used in the analysis. Tables 5-8 list the stability and control parameters for both the rigid and elastic airplane as output by FLEXSTAB. The elastic airplane parameters are shown for both the "free-free structure" and the "fixed-free structure". The free-free airplane analysis is programmed in the FLEXSTAB code. The elastic displacements and rotations in the free-free analysis are with respect to a mean axis system with the origin selected at the aircraft mass center. The elastic distortions relative to a mean-axis system correspond to those of the actual unrestrained flight vehicle and do not contribute to the linear and angular momenta of the relative motion with

respect to the body axes. Hence, the origin of the body axes remains at the aircraft mass center at every instant and reduces the inertial coupling between the overall and relative deformation motions. The fixed-free airplane analysis consists of using a cantilevered (clamped) flexibility matrix which contains implicitly the inertial relief effects. The fixed-free airplane analysis was patched into the FLEXSTAB code for this example to illustrate the significance of the mean-axis formulation. The fixed-free type of solution is sometimes used in present aircraft design, but the free-free solution is more representative of the airplane in flight. Tables 5-8 show the effects of using the free-free analysis. The difference between the free-free and fixed-free analyses for the trim α ($\Delta\alpha$ =0.800°) represents the angle through which the mean axis rotates relative to the clamped axis. The effect of this rotation can be significant for the stability derivatives as presented in tables 6 and 7.

YF-12A

A comparison between the FLEXSTAB predicted and flight measured deformed shape of the YF-12A is shown in figure 10. These results are for a load factor of 1 at a Mach number of 2.8. For this flight condition the agreement is generally good. At subsonic Mach numbers there is not such good agreement. This is probably due to the chine induced vortex flows which FLEXSTAB cannot model.

Arrow-Wing-Body Configuration

Reference 7 presents comparisons of theoretical and experimental transonic pressure distributions for an arrow-wing-body configuration. Example results at M=0.85 for α = 2.1° and 7.9° are given in figure 11 for 2 spanwise locations. In addition to wind tunnel results, 2 sets of analytic potential flow results are shown; one of these is from FLEXSTAB and the other is from Boeing program TEA-230. The FLEXSTAB results for the individual upper and lower surface pressures were computed from a Boeing modified version of FLEXSTAB. The released version of FLEXSTAB computes only the pressure difference between the lower and upper surfaces (lifting pressure).

At α = 2.1° both FLEXSTAB and TEA-230 predict pressure distributions which compare well with the experimental results. In contrast to the mean surface paneling method used in FLEXSTAB, the TEA-230 model employs on-the-surface paneling and boundary conditions. This feature enables the actual wing leading-edge pressures to be more closely predicted by TEA-230 than by FLEXSTAB.

At α = 7.9° the presence of a vortex spiraling off the wing leading edge alters the pressure distribution over a major portion of the wing. As seen in figure 11 the analytic results still agree with experiment at the inboard station but not at the outboard station. This is because neither of the two analytic methods can model the leading-edge vortex flow.

Boeing Fixed-Wing SST

FLEXSTAB and wind tunnel comparisons for the Boeing Fixed-Wing Supersonic Transport (B2707-300) are shown in figure 12. These analytic results were computed from an early version of FLEXSTAB. The figure shows the variation in lift-curve slope and aerodynamic center with Mach number. Agreement between the measured and FLEXSTAB predicted results is good. For supersonic Mach numbers the aerodynamic center predicted by FLEXSTAB tends to be slightly aft of the measured locations, and the lift curve slope tends to be slightly high.

Space Shuttle Orbiter

Figures 13 and 14 show comparisons of pitching moment coefficients due to pitch rate $c_{m_{\hat{q}}}$ (table 3) and due to rate of change of angle of attack $c_{m_{\dot{\hat{\alpha}}}}$ (table 4) for the Space Shuttle Orbiter. Wind tunnel values for the sum $(c_{m_{\hat{q}}} + c_{m_{\dot{\hat{\alpha}}}})$ are compared to FLEXSTAB computed values in figure 13. The agreement is remarkably good considering the unstreamlined shape of the Orbiter. In contrast to wind tunnel measurements in which only the sum $c_{m_{\hat{q}}} + c_{m_{\dot{\hat{\alpha}}}}$ is generally measured, FLEXSTAB computes each derivative separately. These are shown in figure 14 where it is seen that $c_{m_{\dot{\hat{\alpha}}}}$ is destabilizing at the supersonic Mach number.

LEVEL 1 FLEXSTAB DOCUMENTATION, AVAILABILITY AND IMPLEMENTATION

The documentation for Level 1 FLEXSTAB is listed under references 1 and 2.

Both a CDC and an IBM version of the NASA FLEXSTAB Program are available from COSMIC through a lease arrangement. Inquiries concerning the lease should be made to:

Computer Software Management and Information Center
Barrow Hall
University of Georgia
Athens, Georgia 30601

The CDC version has been executed on the following computers, using FORTRAN Extended compilers:

1. CYBER 70, Model 73, SCOPE 3.4 Operating System

2. CDC 6600, KRONOS 2.1 and SCOPE 3.4 Operating Systems

3. CDC 7600, SCOPE 2.1.3 Operating System

The IBM version requires both the G and H compilers and has been executed on the following computers:

1. IBM 360-91/OS

2. IBM 360-67/OS

Additional information on the program implementation requirements is summarized in reference 1.

LEVEL 2 FLEXSTAB CAPABILITIES

The Air Force has developed additional capabilities for FLEXSTAB for the evaluation of the low frequency dynamics of control configured vehicles (ref. 3). These capabilities are subject to the same limitations as Level 1 FLEXSTAB imposed by the structural modeling and the low frequency aerodynamic approximation. The additional capabilities can be summarized as:

- Active Controls Capability
- User Specification of Linear Control System
- Sensor Simulations
- Time Histories of Controlled Airplane
- RMS Aircraft Motion Due to Turbulence PSD
- Frequency Response Calculations
- Structural Damping
- Modal Truncation Formulation for the Structural Dynamic Model
- Plotting of Dynamic Analysis Data
- Data Interface For Flight Simulators
- Fore and Aft Gust Capability
- Aerodynamic Hinge Moments

This extended capability of FLEXSTAB allows the analytical representation of arbitrary combinations of active control systems and linear systems analysis of the response to turbulence and control commands. Nonlinear response to discrete gusts and control commands may also be evaluated by time histories generated by the system.

The functional configuration of the Level 2 FLEXSTAB system is shown in figure 15. The program system totals twelve separate programs with about 140 000 source statements. Five of the programs remain the same as for Level 1 FLEXSTAB, six have been modified, mainly to allow definition of motions at the sensor locations used by the flight control system, and one program, the linear system analysis, is new.

The program has been used by the Air Force for research on the following aircraft; YF-16, B-1, C-5A, and the F-111 TACT. Also the program is being used in a preliminary design mode of operation for system integration in support of fire control systems on the airborne laser weapons program.

Figure 16 shows a typical result from Level 2 FLEXSTAB for the B-52E aircraft response to a lateral gust with and without a yaw stability augmentation system (yaw SAS).

LEVEL 2 FLEXSTAB DOCUMENTATION, AVAILABILITY AND IMPLEMENTATION

The documentation for Level 2 FLEXSTAB is listed under reference 3. The program is available only for application to Department of Defense problems from the Air Force by sending a request to:

AFFDL
Flight Control Division
Wright-Patterson Air Force Base
Ohio 45433

The Level 2 version has been executed on the CYBER 74 and CDC 6600 under the KRONOS 2.0 and 2.1, SCOPE 3.4 and NOS/BE Operating Systems.

CONCLUDING REMARKS

The development of the Level 1 FLEXSTAB computer program system provides a first generation program to partially satisfy the requirement for an automated aeroelastic analysis tool. The system is based on integrated aerodynamic, structural, and dynamic analytical methods applicable to aircraft configurations having a plane of symmetry. The aerodynamic analysis may be supplemented or modified with empirical data. Also the system includes the low frequency aerodynamic effects appropriate for evaluating the stability of large aircraft.

Through application to several different aircraft configurations it has been shown that the linearized theory employed is capable of providing aeroelastic analysis of complex configurations. The linearized theory provides good correlation with experiment as long as the flow over the configuration remains attached, although in some cases it may also provide useful data for separated flow conditions. Further work is required to develop methods of representing leading-edge vortex flow.

The Level 2 system integrates the aerodynamic and structural methods used in Level 1 with control system dynamics. The resulting system is capable of analyzing the static and low frequency dynamic characteristics of control configured vehicles.

By refining the structural modeling and providing full unsteady aerodynamic capability, the FLEXSTAB system could be applied to prediction of dynamic loads at higher structural frequencies.

REFERENCES

1. Tinoco, E. N.; and Mercer, J. E.: FLEXSTAB - A Summary of the Functions and Capabilities of the NASA Flexible Airplane Analysis Computer System. NASA CR-2564, 1975.

2. Boeing Commer. Airplane Co.: A Method for Predicting the Stability Characteristics of an Elastic Airplane.

   a. Vol. I - FLEXSTAB Theoretical Description, NASA CR-114712, 1974
   b. Vol. II - FLEXSTAB 1.02.00 User's Manual, NASA CR-114713, 1974
   c. Vol. III - FLEXSTAB 1.02.00 Program Description, NASA CR-114714, 1974
   d. Vol. IV* - FLEXSTAB 1.02.00 Demonstration Cases and Results, NASA CR-114715, 1974.

3. Boeing Commer. Airplane Co.: A Method for Predicting the Stability Characteristics of Control Configured Vehicles. AFFDL-TR-74-91, 1974.

   a. Vol. I - FLEXSTAB 2.01.00 Theoretical Description
   b. Vol. II - FLEXSTAB 2.01.00 User's Manual
   c. Vol. III - FLEXSTAB 2.01.00 Programmer's Manual
   d. Vol. IV - FLEXSTAB 2.01.00 B-52E LAMS Demonstration Case and Results

4. Woodward, F. A.: Analysis and Design of Wing-Body Combinations at Subsonic and Supersonic Speeds. Journal of Aircraft, Vol. 5, No. 6, November-December, 1968, pp 528-534.

5. Rubbert, P. E., "Sideslip of Wing-Body Combinations", NASA CR-114716, 1975.

6. Preliminary Design Dep., Boeing Commer. Airplane Co.: Study of Structural Design Concepts for an Arrow Wing Supersonic Transport Configuration. Vols. 1 and 2. NASA CR-132576, 1976.

7. Manro, M. E., Manning, K.J.R., Hallstaff, T. H., Rogers, J. T., Transonic Pressure Measurements and Comparison of Theory to Experiment for an Arrow-Wing Configuration. Vol. III: Data Report — Comparison of Attached Flow Theories to Experiment. NASA CR-132729, 1975.

---

* Not yet released. Preliminary copies available from NASA Ames Research Center.

Symbols used in Table 1 and Figure 8

EI	beam flexural rigidity
GJ	beam torsional rigidity
[LSC]	steady lifting aerodynamic influence coefficient matrix
P, Q, R	components of angular velocity, ω
u, v, w	perturbation components of velocity
ρ	density of air
θ, ϕ, ψ	Euler angles

Subscripts:

1	reference state

Superscripts:

• (dot)	first derivative with respect to time

TABLE 1.- PROGRAMS OF THE LEVEL 1 FLEXSTAB SYSTEM

No.	Program Title	Program Name	Purpose	Data Flow	
				Input	Output
AIRPLANE MODELING SECTION					
1	Geometry definition program	GD	To geometrically construct an airplane configuration that complies with the requirements of the aerodynamic and structural theories	• Basic geometric description of the airplane (wing planform, airfoil shapes, wing twist, body radius distribution, body camber, etc.) in its cruise or unload condition	• Geometric defining quantities required for a linearized aerodynamic and structural representation (such as panel corner points and location of line doublet segments) CalComp plots of the airplane's configuration
2	Aerodynamic influence coefficient program	AIC	To produce matrices that relate the change in pressure on a panel to the change in flow incidence at another panel $A_{ij} = \frac{\partial P_i}{\partial \psi_j}$ and to produce matrices that relate the change in pressure on a panel to the rate of change in flow incidence at another panel $\delta A_{ij} = \frac{\partial P_i}{\partial \dot{\psi}_i}$	• Mach number • Geometric defining quantities produced by the GD program	• Aerodynamic influence coefficient (AIC) matrices
3	AIC matric correction program	CAIC	To correct the [LSC] AIC matrix using (a) a correction matrix $[C_2]$ based on wind tunnel or flight-test data (b) a replacement technique in which the user specifies elements of the matrix	• The [LSC] AIC matrix	• A corrected [LSC] matrix

TABLE 1.- CONTINUED

No.	Program Title	Program Name	Purpose	Data Flow	
				Input	Output
	STRUCTURAL MODELING SECTION				
4	Internal structural influence coefficient program	ISIC	To produce flexibility matrices based on beam theory and consistent with paneling used for computing the AIC matrices	•Geometric defining quantities produced by the GD program •Elastic axis geometric description •EIs and GJs of beam segments •Mass distribution	•Flexibility matrices (Static-elastic) •Mass matrix
5	Elastic axis plot program	EAPLOT	To plot the structural elastic axes	•Elastic axis data	•CalComp plots of the airplane's elastic axis
6	Normal modes program	NM	To calculate the free-vibration normal mode shapes and then to construct normal mode matrices	•Number of normal modes requested •Structural (ISIC) flexibility matrices	•Mode shape matrices •Residual flexibility matrices
7	Normal modes plot program	NMPLOT	To plot the normal mode shapes	•Normal mode shapes	•CalComp plots of the mode shapes
8	External structural influence coefficient program	ESIC	To accept a flexibility matrix from a source external to the FLEXSTAB system and by interpolation produce a new flexibility matrix consistent with paneling used for computing the AIC matrices	•Geometric defining quantities produced by the GD program •Structural mode shapes •External flexibility matrix	•New flexibility matrices •Mass matrix •Normal mode matrices

TABLE 1.- CONCLUDED

No.	Program Title	Program Name	Purpose	Data Flow	
				Input	Output
	PROBLEM ANALYSIS SECTION				
9	Stability derivatives and static stability program	SD&SS	To calculate the static and dynamic stability characteristics of the airplane	•Geometric defining quantities produced by the GD program •AIC matrices •Flexibility matrices •Normal mode matrices •Flight condition (altitude, ρ, P_1, R_1, Q_1, ϕ, γ_1, T_1) •Wind tunnel data •Exterior downwash data	•Trim parameters (α_1, δ_{e_1}, T_1, β_1, δ_{a_1}, and δ_{r_1} •Deformed shape •Steady and unsteady pressure distribution •Static and dynamic stability derivatives •Static stability parameters (static margin, neutral point, etc.) •Control effectiveness
10	Pressure distribution plot program	PDPLOT	To plot the steady and unsteady pressure distributions	•Steady or unsteady pressure distribution	•CalComp plots of the pressure distribution
11	Time histories program	TH	To help the user evaluate the stability of an airplane using large-disturbance theory (nonlinear equations)	•Geometric data •Dynamic stability derivatives •Stability data (α_1, β_1, ϕ_1, γ_1, etc.) •Wind tunnel data	•Values of motion variables versus time of flight (u, v, w, $\dot{u}$, $\dot{v}$, $\dot{w}$, θ, ϕ, ψ, $\dot{\theta}$, $\dot{\phi}$, $\dot{\psi}$, etc.)
12	Time histories plot program	THPLOT	To plot the time histories (motion variables versus time) of the flight	•Motion variables versus time	•CalComp plots of the time histories
13	Structural loads program	SLOADS	To print the structural elastic axis loads	•Structural load matrices	•Structural loads on elastic axis
14	Aerodynamic loads	ALOADS	To calculate air loads	• Air load matrices	•Air loads

TABLE 2.- STATIC STABILITY AND TRIM PARAMETERS

TRIM PARAMETERS	
α	angle of attack
β	angle of sideslip
δ_e	elevator deflection angle
δ_a	aileron deflection angle
δ_r	rudder deflection angle
T	thrust
γ	flightpath angle
TRIMMED FORCE COEFFICIENTS	
C_L	lift coefficient
C_D	drag coefficient
C_m	pitching moment coefficient
C_y	sideforce coefficient
C_ℓ	rolling moment coefficient
C_n	yawing moment coefficient
STATIC STABILITY PARAMETERS	
h_n-h	static margin
h_n	neutral point
h_m-h	maneuver margin
$\partial\delta_e/\partial n \left(=\frac{\Delta\delta_e}{n-1}\right)$	elevator angle per g (turn, pullup)
$\partial\delta_e/\partial V$	speed stick stability

TABLE 3.- STATIC STABILITY DERIVATIVES AND CONTROL EFFECTIVENESS COEFFICIENTS

C_{L_o}	lift coefficient at $\alpha = \delta_e = 0$	$C_{n_{\hat{p}}}$	yawing moment coefficient due to roll rate
C_{D_o}	drag coefficient at $\alpha = \delta_e = 0$	$C_{y_{\hat{r}}}$	sideforce coefficient due to yaw rate
C_{m_o}	pitching moment coefficient at $\alpha = \delta_e = 0$	$C_{\ell_{\hat{r}}}$	rolling moment coefficient due to yaw rate
C_{L_α}	lift coefficient due to angle of attack	$C_{n_{\hat{r}}}$	yawing moment coefficient due to yaw rate
C_{D_α}	drag coefficient due to angle of attack	C_{y_β}	sideforce coefficient due to sideslip
C_{m_α}	pitching moment coefficient due to angle of attack	C_{ℓ_β}	rolling moment coefficient due to sideslip
$C_{L_{\hat{q}}}$	lift coefficient due to pitch rate	C_{n_β}	yawing moment coefficient due to sideslip
$C_{D_{\hat{q}}}$	drag coefficient due to pitch rate	$C_{y_{\delta_a}}$	sideforce coefficient due to aileron deflection (antisymmetrically deflected)
$C_{m_{\hat{q}}}$	pitching moment coefficient due to pitch rate	$C_{\ell_{\delta_a}}$	rolling moment coefficient due to aileron deflection (antisymmetrically deflected)
$C_{L_{\delta_e}}$	lift coefficient due to elevator deflection	$C_{n_{\delta_a}}$	yawing moment coefficient due to aileron deflection (antisymmetrically deflected)
$C_{D_{\delta_e}}$	drag coefficient due to elevator deflection	$C_{y_{\delta_r}}$	sideforce coefficient due to rudder deflection
$C_{m_{\delta_e}}$	pitching moment coefficient due to elevator deflection	$C_{\ell_{\delta_r}}$	rolling moment coefficient due to rudder deflection
$C_{y_{\hat{p}}}$	sideforce coefficient due to roll rate	$C_{n_{\delta_r}}$	yawing moment coefficient due to rudder deflection
$C_{\ell_{\hat{p}}}$	rolling moment coefficient due to roll rate		

TABLE 4.- DYNAMIC STABILITY DERIVATIVES AND CONTROL EFFECTIVENESS COEFFICIENTS

$C_{L_{\hat{\dot{\alpha}}}}$	lift coefficient due to angle-of-attack rate
$C_{D_{\hat{\dot{\alpha}}}}$	drag coefficient due to angle-of-attack rate
$C_{m_{\hat{\dot{\alpha}}}}$	pitching moment coefficient due to angle-of-attack rate
$C_{L_{\hat{u}}}$	lift coefficient due to speed change
$C_{D_{\hat{u}}}$	drag coefficient due to speed change
$C_{m_{\hat{u}}}$	pitching moment coefficient due to speed change
$C_{L_{\hat{q}}}$	lift coefficient due to pitch acceleration
$C_{D_{\hat{q}}}$	drag coefficient due to pitch acceleration
$C_{m_{\hat{q}}}$	pitching moment coefficient due to pitch acceleration
$C_{y_{\hat{\dot{p}}}}$	sideforce coefficient due to roll acceleration
$C_{\ell_{\hat{\dot{p}}}}$	rolling moment coefficient due to roll acceleration
$C_{n_{\hat{\dot{p}}}}$	yawing moment coefficient due to roll acceleration
$C_{y_{\hat{\dot{r}}}}$	sideforce coefficient due to yaw acceleration
$C_{\ell_{\hat{\dot{r}}}}$	rolling moment coefficient due to yaw acceleration
$C_{n_{\hat{\dot{r}}}}$	yawing moment coefficient due to yaw acceleration
$C_{y_{\hat{\beta}}}$	sideforce coefficient due to sideslip rate
$C_{\ell_{\hat{\beta}}}$	rolling moment coefficient due to sideslip rate
$C_{n_{\hat{\beta}}}$	yawing moment coefficient due to sideslip rate
$C_{L_{\dot{\delta}_e}}$	lift coefficient due to elevator deflection rate
$C_{D_{\dot{\delta}_e}}$	drag coefficient due to elevator deflection rate
$C_{m_{\dot{\delta}_e}}$	pitching moment coefficient due to elevator deflection rate
$C_{y_{\dot{\delta}_a}}$	sideforce coefficient due to aileron deflection rate (antisymmetric deflection)
$C_{\ell_{\dot{\delta}_a}}$	rolling moment coefficient due to aileron deflection rate (antisymmetric deflection)
$C_{n_{\dot{\delta}_a}}$	yawing moment coefficient due to aileron deflection rate (antisymmetric deflection)
$C_{y_{\dot{\delta}_r}}$	sideforce coefficient due to rudder deflection rate
$C_{\ell_{\dot{\delta}_r}}$	rolling moment coefficient due to rudder deflection rate
$C_{n_{\dot{\delta}_r}}$	yawing moment coefficient due to rudder deflection rate

TABLE 5.- NASA ARROW-WING SUPERSONIC CRUISE AIRCRAFT STATIC STABILITY AND TRIM PARAMETERS

	Free-Free Airplane		Fixed-Free Airplane
	Rigid	Static-Elastic	Static-Elastic
Trim parameters			
α_1 deg.	5.318	5.441	6.241
β_1 deg.	0	0	0
δ_{e_1} deg.	2.298	14.156	14.156
δ_{a_1} deg.	0	0	0
δ_{r_1} deg.	0	0	0
T_1 lb.	144 000	144 000	144 000
γ_1 deg.	7.319	7.349	6.549
Static stability parameters			
h_n-h	0.0983	0.0183	0.0183
h_n	0.6213	0.5413	0.5413
h_m-h	0.1010	0,0205	0.0205
$\partial\delta_e/\partial n \left(=\frac{\Delta\delta_e}{n-1}\right)$ deg./g	-8.000	-2.416	-2.421
$\partial\delta_e/\partial v$ deg./ft/sec.	0.0070	0.0010	0.0010

Weight = 298 636 Kg (657 000 lb) C_L = 0.0666 M = 2.9 C.G = 0.523 $\bar{c}$ h = 17 435 m (57 200 ft)

TABLE 6.- NASA ARROW-WING SUPERSONIC CRUISE AIRCRAFT STATIC STABILITY DERIVATIVES AND CONTROL EFFECTIVENESS COEFFICIENTS

	Free-Free Airplane		Fixed-Free Airplane
	Rigid	Static-Elastic	Static-Elastic
C_{L_o}	-0.090394	-0.087729	-0.093639
C_{D_o}	0.004326	0.004246	0.004306
C_{m_o}	0.016662	0.010725	0.010831
C_{L_α}/deg.	0.029008	0.026645	0.023918
C_{D_α}/deg.	0.003038	0.002916	0.002955
C_{m_α}/deg.	-0.002851	-0.000486	-0.000438
$C_{L_{\hat{q}}}$/rad.	0.636205	0.345434	0.500099
$C_{D_{\hat{q}}}$/rad.	0.068107	0.047567	0.072209
$C_{m_{\hat{q}}}$/rad.	-0.881881	-0.727361	-0.730188
$C_{L_{\delta_e}}$/deg.	0.000939	0.000568	0.000804
$C_{D_{\delta_e}}$/deg.	0.000059	0.000046	0.000780
$C_{m_{\delta_e}}$/deg.	-0.000918	-0.000566	-0.000570
$C_{y_{\hat{p}}}$/rad.	-0.002286	-0.001445	0.006297
$C_{\ell_{\hat{p}}}$/rad.	-0.133523	-0.099685	-0.100626
$C_{n_{\hat{p}}}$/rad.	0.006054	0.005165	0.004863
$C_{y_{\hat{r}}}$/rad.	0.219438	0.128576	0.172671
$C_{\ell_{\hat{r}}}$/rad.	-0.007389	-0.018225	-0.025462
$C_{n_{\hat{r}}}$/rad.	-0.167888	-0.114434	-0.122142
C_{y_β}/deg.	-0.003305	-0.001722	-0.002574
C_{ℓ_β}/deg.	0.000038	0.000214	0.000327
C_{n_β}/deg.	0.001279	0.000292	0.000443
$C_{y_{\delta_a}}$/deg.	-0.0	0.000010	0.000013
$C_{\ell_{\delta_a}}$/deg.	-0.000115	-0.000057	-0.000057
$C_{n_{\delta_a}}$/deg.	0.000011	0.000003	0.000004
$C_{y_{\delta_r}}$/deg.	0.000228	0.000071	0.000163
$C_{\ell_{\delta_r}}$/deg.	-0.000002	0.000015	0.000003
$C_{n_{\delta_r}}$/deg.	-0.000172	-0.000069	-0.000086

TABLE 7.- NASA ARROW-WING SUPERSONIC CRUISE AIRCRAFT DYNAMIC STABILITY DERIVATIVES

	Free-Free Airplane		Fixed-Free Airplane
	Rigid	Static-Elastic	Static-Elastic
$C_{L_{\hat{\alpha}}}$/rad	-0.048826	0.064902	0.244706
$C_{D_{\hat{\alpha}}}$/rad	-0.006662	0.004098	0.024072
$C_{m_{\hat{\alpha}}}$/rad	0.058374	-0.021734	-0.024995
$C_{L_{\hat{u}}}$	0.064077	0.068511	0.045412
$C_{D_{\hat{u}}}$	0.005153	0.059110	0.004428
$C_{m_{\hat{u}}}$	0.008657	0.007856	0.008273
$C_{L_{\hat{q}}}$/rad	-0.280092	0.345434	0.500099
$C_{D_{\hat{q}}}$/rad	-0.015575	0.047567	0.072209
$C_{m_{\hat{q}}}$/rad	-0.062581	-0.727361	-0.730188
$C_{y_{\hat{p}}}$/rad	-0.021108	-0.011722	-0.020624
$C_{\ell_{\hat{p}}}$/rad	0.009710	-0.003486	-0.002221
$C_{n_{\hat{p}}}$/rad	0.014685	0.008969	0.010627
$C_{y_{\hat{r}}}$/rad	-0.043381	-0.031054	-0.040741
$C_{\ell_{\hat{r}}}$/rad	-0.043000	-0.009016	-0.008496
$C_{n_{\hat{r}}}$/rad	-0.043619	-0.051572	-0.049689
$C_{y_{\hat{\beta}}}$/rad	-0.059523	-0.058859	-0.059655
$C_{\ell_{\hat{\beta}}}$/rad	-0.002412	-0.001590	-0.001705
$C_{n_{\hat{\beta}}}$/rad	-0.015210	-0.015543	-0.015375

TABLE 8.- NASA ARROW-WING SUPERSONIC CRUISE AIRCRAFT LONGITUDINAL AND LATERAL DIRECTIONAL DYNAMIC CHARACTERISTICS

$M_1 = 2.9$, $h_1 = 17\,435$ m (57 200 ft), $\gamma_1 = 7.3°$, cg = $0.523\bar{c}$, wt = 298 636 Kg (657 000 lb)

V = 1015 km/hr (548 keas)

		Short Period			Phugoid		
		Period (sec)	$T_{1/2}$ or T_2* (sec)	$C_{1/2}$ or C_2* (cycles)	Period (sec)	$T_{1/2}$ or T_2* (sec)	$C_{1/2}$ or C_2* (cycles)
Free-Free Airplane	Rigid	3.55	$T_{1/2} = 2.44$	$C_{1/2} = 0.687$	368.3	$T_2 = 28\,904$	$C_2 = 78.5$
	Static-elastic	8.54	$T_{1/2} = 2.69$	$C_{1/2} = 0.316$	214.9	$T_{1/2} = 267.8$	$C_{1/2} = 1.25$
Fixed-Free Airplane	Static-elastic	8.99	$T_{1/2} = 2.84$	$C_{1/2} = 0.316$	215.9	$T_{1/2} = 225.7$	$C_{1/2} = 1.05$

		Dutch roll					Roll convergence	Spiral mode
		Period (sec)	$T_{1/2}$ or T_2* (sec)	$C_{1/2}$ or C_2* (cycles)	$\lvert\phi/\beta\rvert$	Phase angle (deg.)	$T_{1/2}$ (sec)	$T_{1/2}$ or T_2 (sec)
Free-Free Airplane	Rigid	4.83	$T_{1/2} = 10.7$	$C_{1/2} = 2.21$	0.22	41.45	$T_{1/2} = 1.36$	$T_2 = 308.0$
	Static-elastic	12.15	$T_{1/2} = 241.3$	$C_{1/2} = 19.85$	5.56	-144.43	$T_{1/2} = 1.49$	$T_2 = 60.7$
Fixed-Free Airplane	Static-elastic	10.23	$T_2 = 107.93$	$C_2 = 10.5$	6.17	-146.74	$T_{1/2} = 1.39$	$T_2 = 61.2$

*Time or cycles to half or twice amplitude.

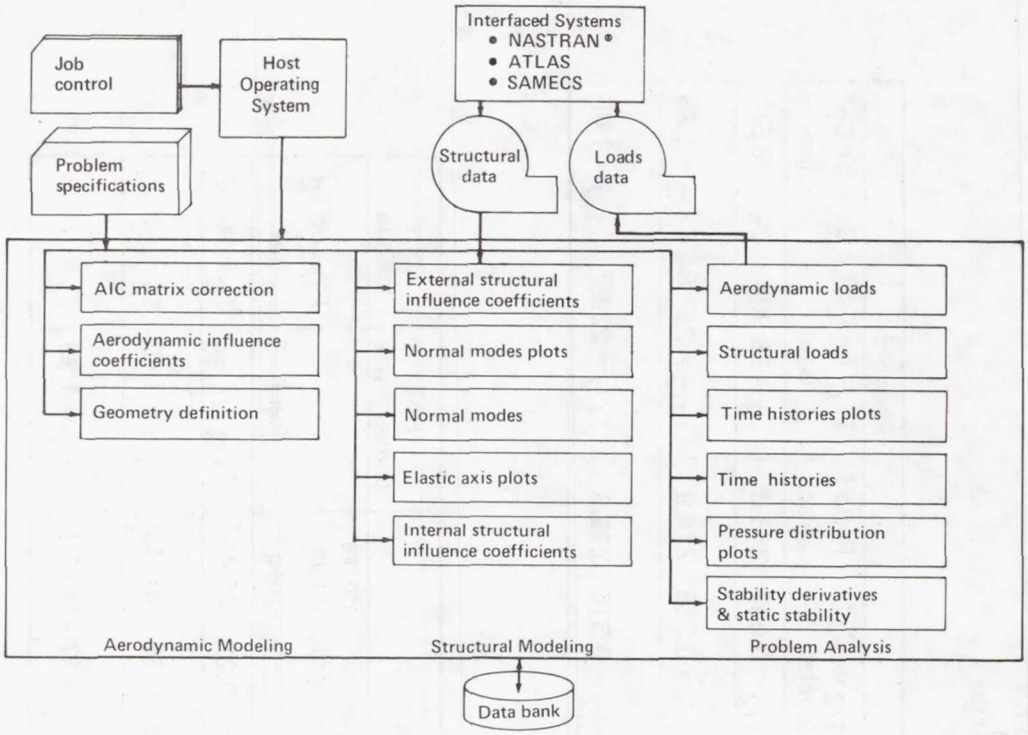

Figure 1.- Level 1 FLEXSTAB functional configuration.

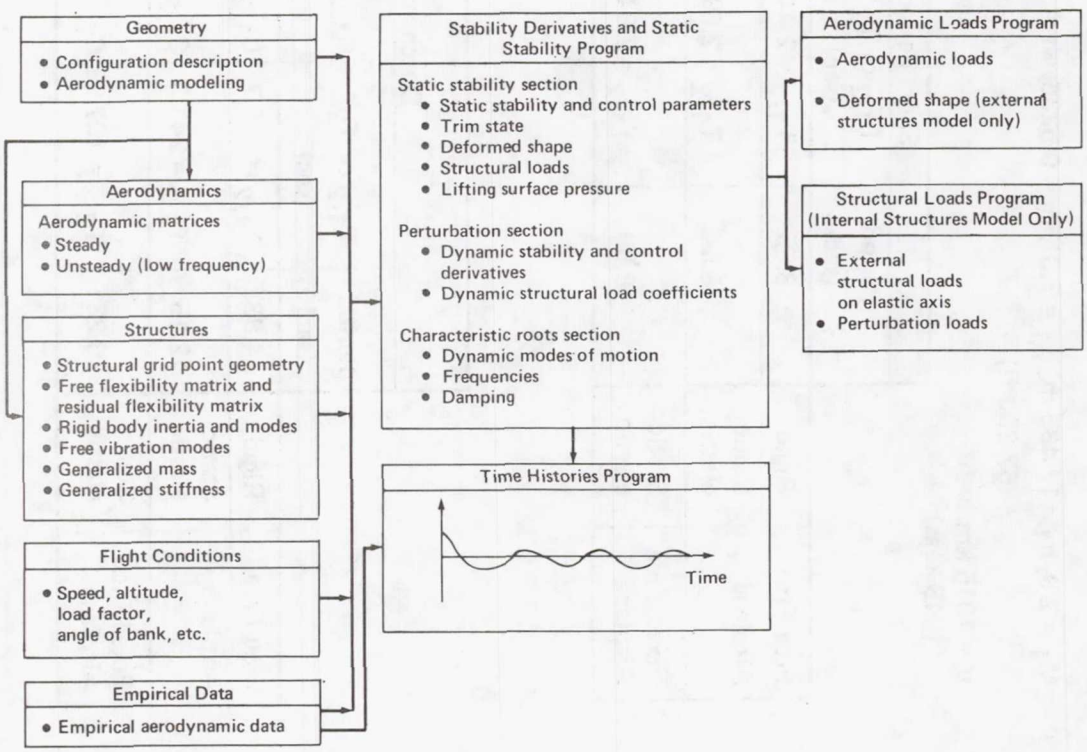

Figure 2.- FLEXSTAB analysis sequence.

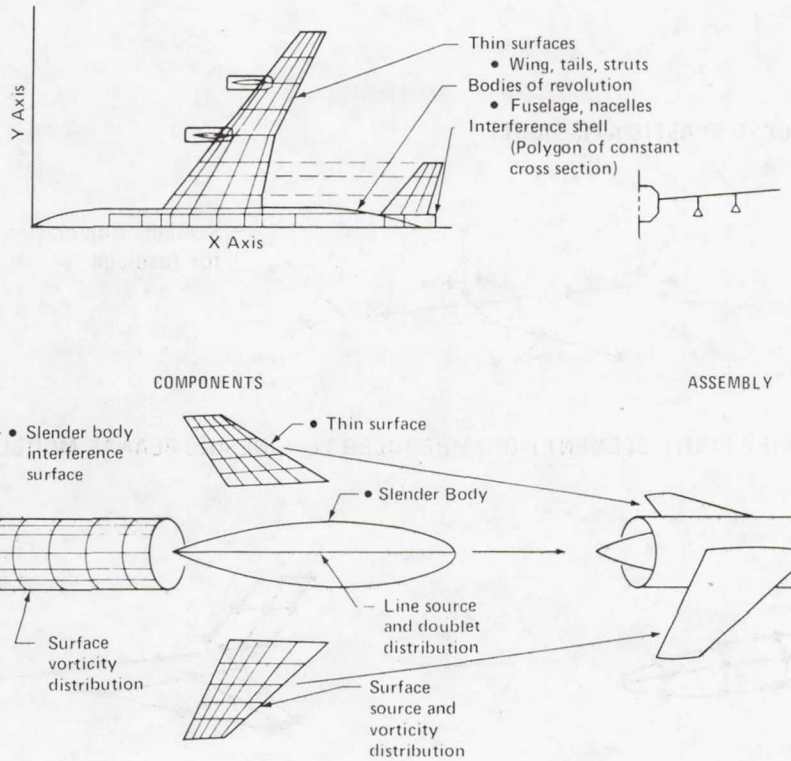

Figure 3.- FLEXSTAB aerodynamic geometry modeling.

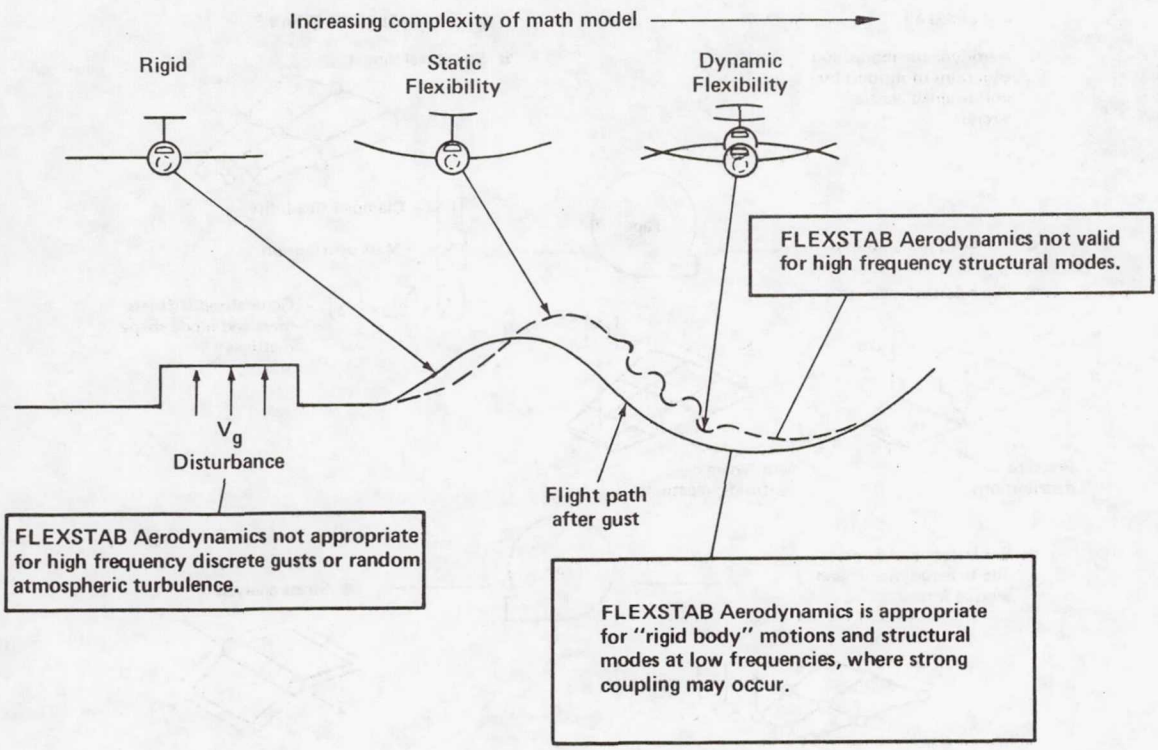

Figure 4.- Limitations on low frequency aerodynamic approximation.

- INTERNALLY PRODUCED ELASTIC AXIS MODEL

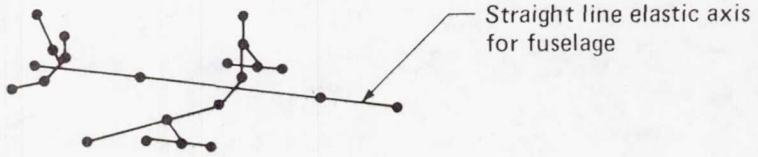

- EXTERNALLY SUPPLIED FINITE ELEMENT MODEL REDUCED TO LINE AND PLANAR MODEL

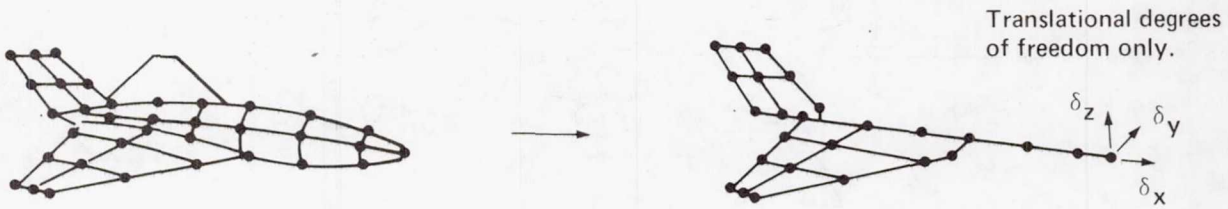

Figure 5.- FLEXSTAB structural modeling.

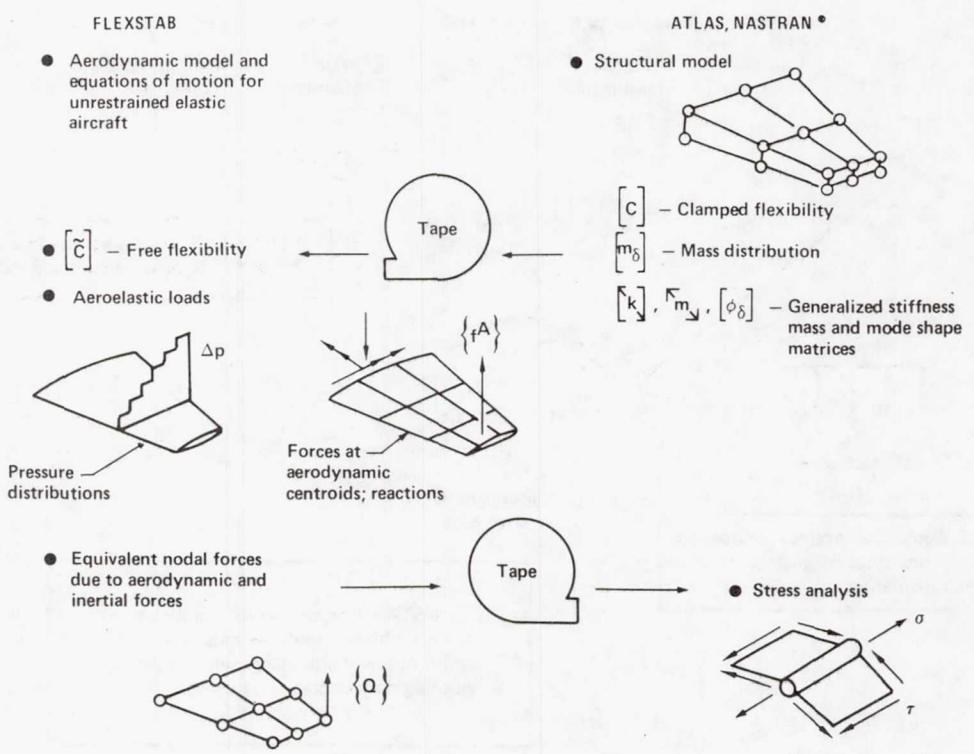

Figure 6.- FLEXSTAB/ATLAS, NASTRAN® interface.

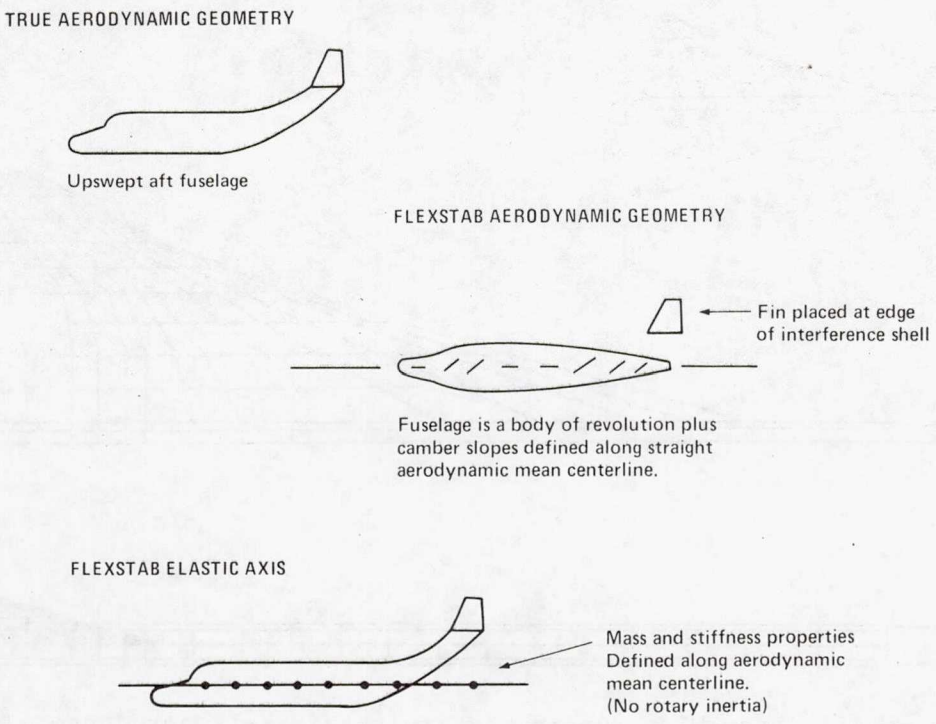

Figure 7.- FLEXSTAB modeling limitations.

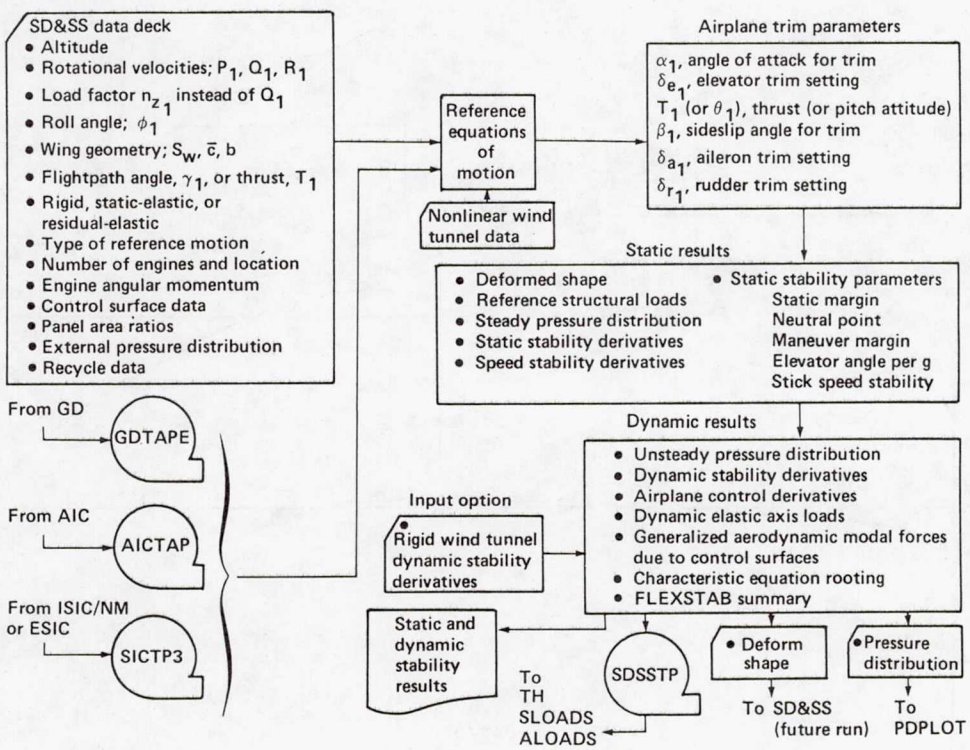

Figure 8.- Schematic of the SD&SS program.

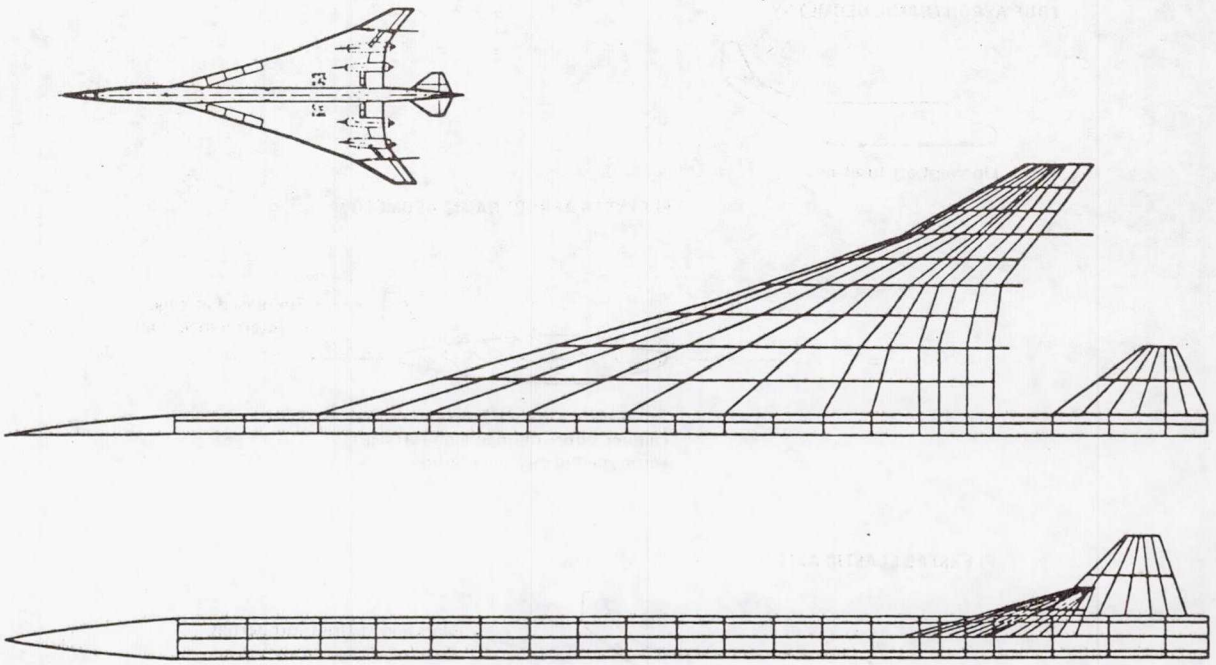

Figure 9.- NASA Arrow-Wing supersonic cruise aircraft aerodynamic peneling.

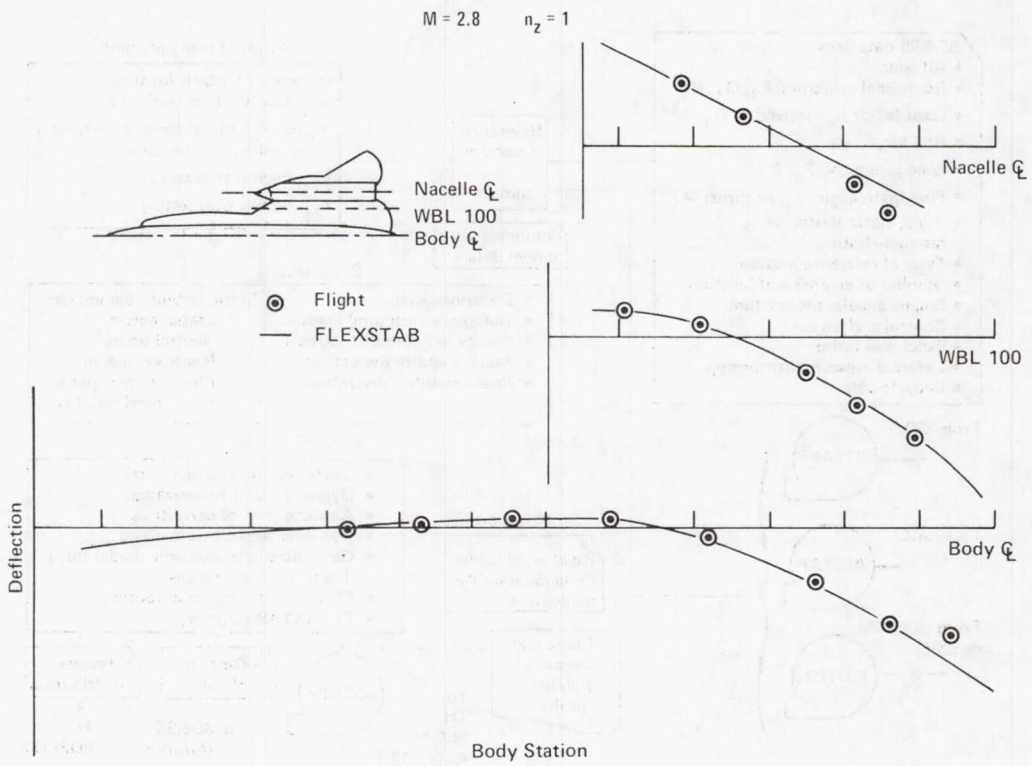

Figure 10.- FLEXSTAB/flight deformed shape of YF-12A.

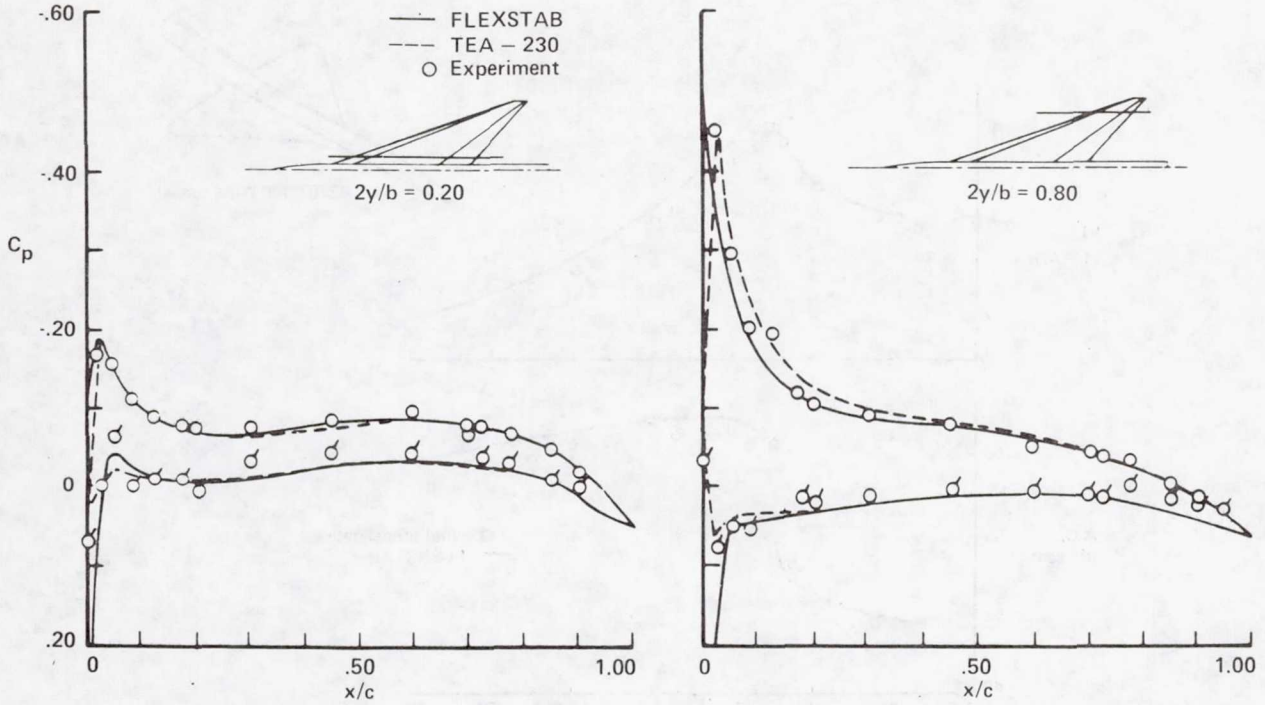

(a) M = 0.85 and $\alpha = 2.1^{o}$.

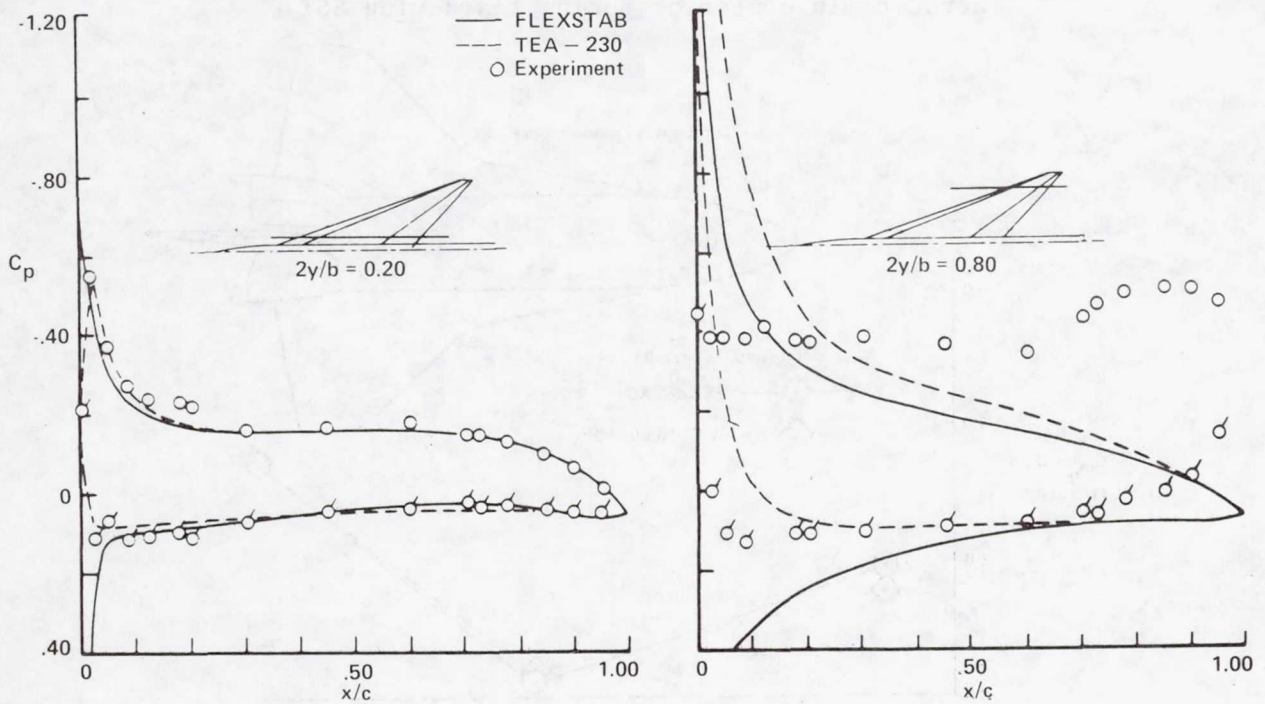

(b) M = 0.85 and $\alpha = 7.9^{o}$.

Figure 11.- Flat wing pressure distribution of Arrow-Wing – body.

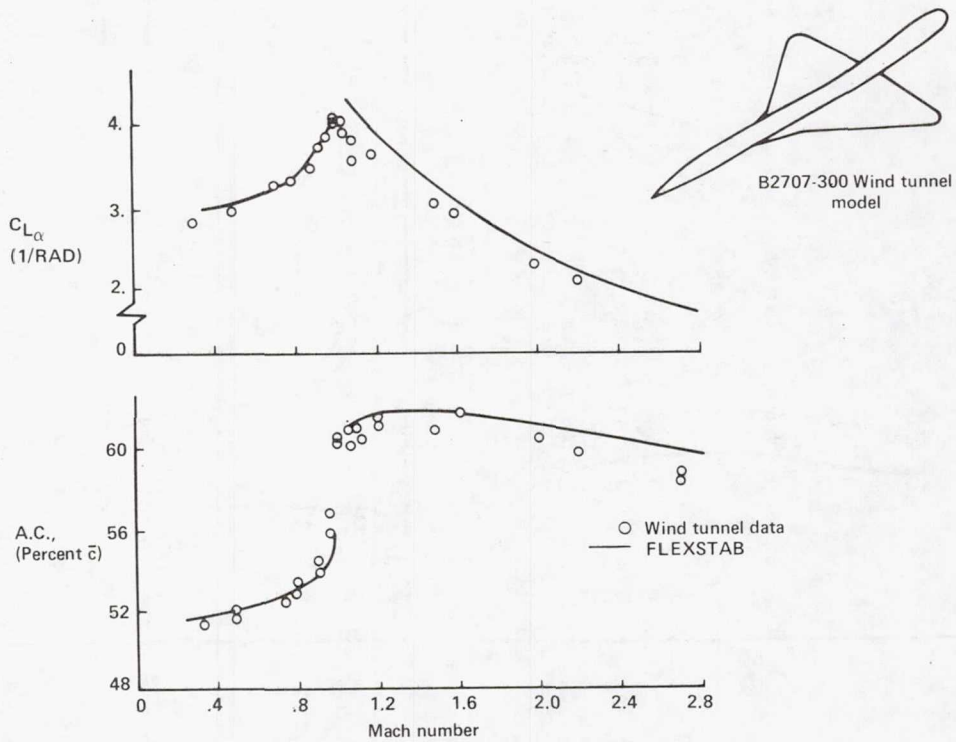

Figure 12.- Effect of Mach number on lift-curve slope and aerodynamic center of Boeing fixed-wing SST.

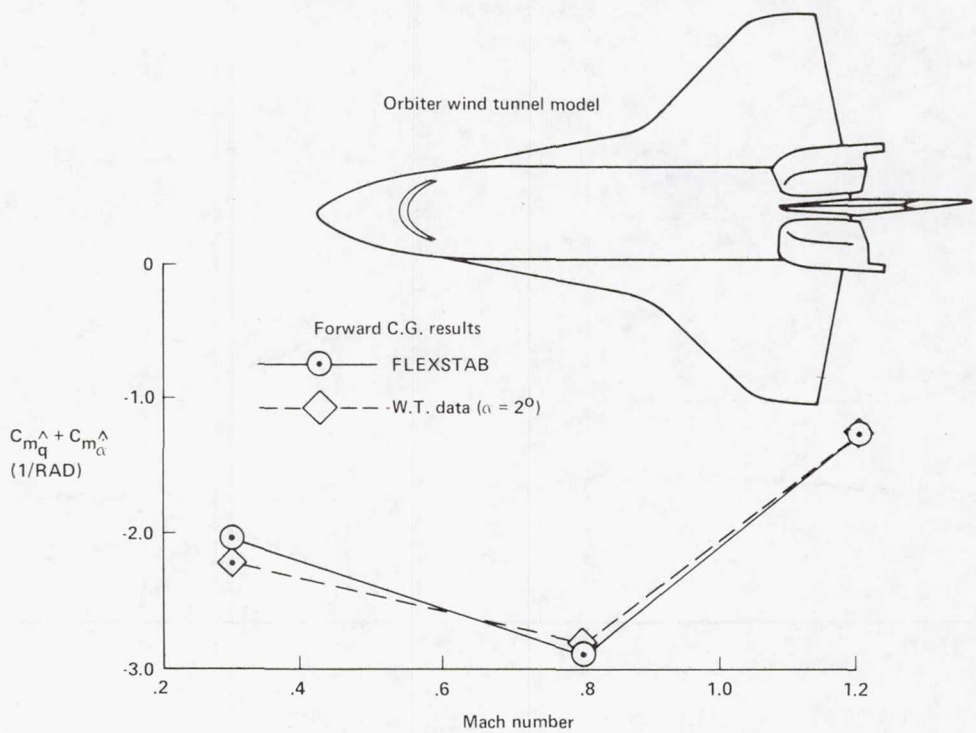

Figure 13.- Space shuttle orbiter values of $C_{m_{\hat{q}}} + C_{m_{\hat{\alpha}}}$.

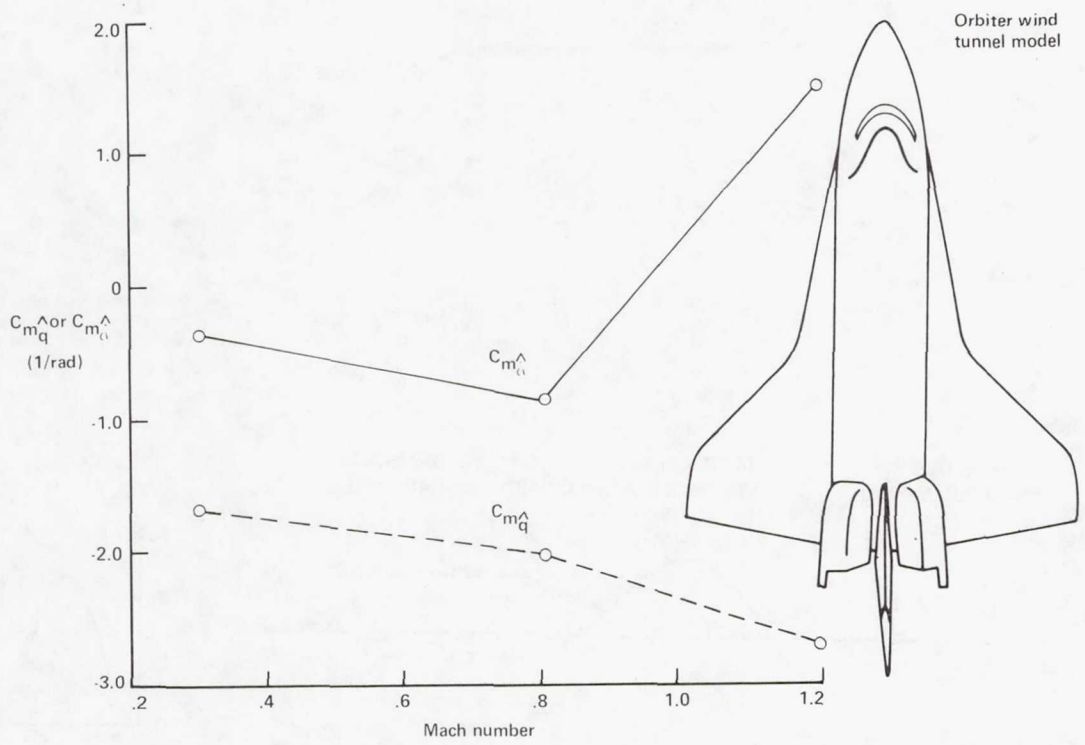

Figure 14.- FLEXSTAB values of $C_{m_{\hat{q}}}$ and $C_{m_{\hat{\dot{\alpha}}}}$.

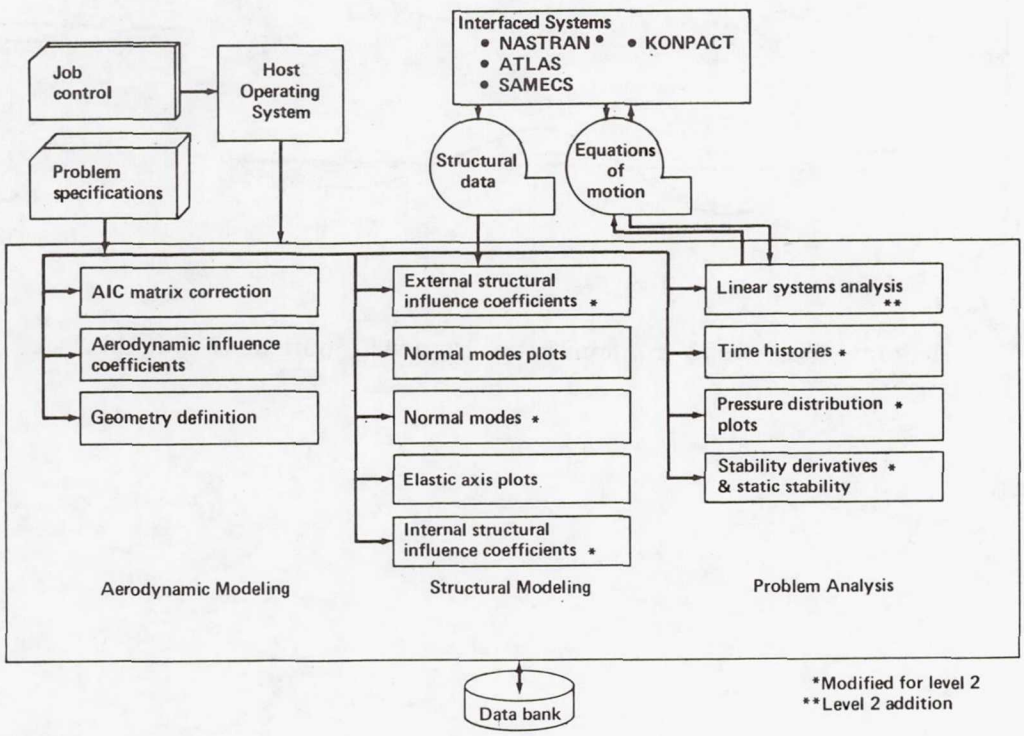

Figure 15.- Level 2 FLEXSTAB functional configuration.

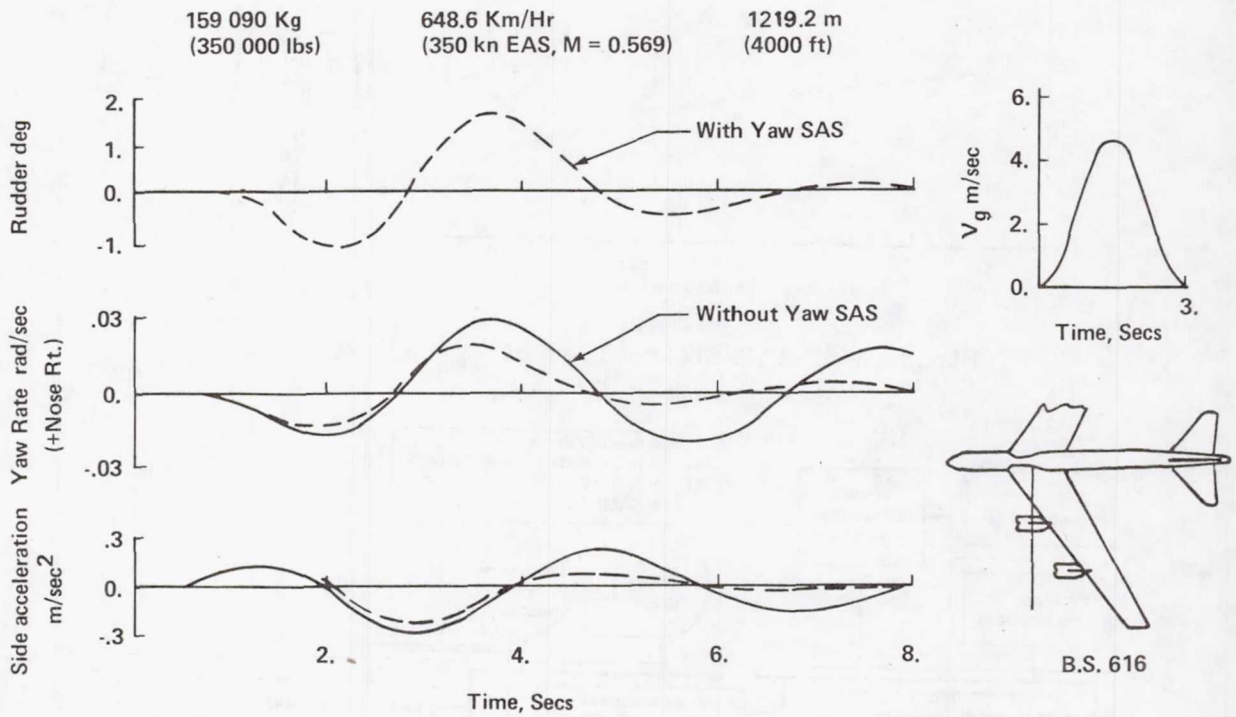

Figure 16.- B-52 response to lateral gust at B.S.616.